Residual impurities on fused silica surface processed by different technics and their effects on laser induced damage at 355nm

LIU HONGJIE[a], HUANG JIN[a], YE XIN[a], SUN LAIXI[a], WANG FENGRUI[a], GENG FENG[a], JIANG XIAODONG[a,*], WU WEIDONG[a,b], ZHENG WANGUO[a]
[a]Research Center of Laser Fusion, China Academy of Engineering Physics, Mianyang 621900, China
[b]IFSA Collaborative Innovation Center, Shanghai Jiao Tong University, Shanghai 200240, China

Laser-induced damage on fused silica surface at fluences and intensities far below the intrinsic damage threshold is often ignited by absorbing impurities introduced by polishing or post processing. This paper reports the residual impurities on fused silica surface under different polishing and post processing conditions and their impacts on laser induced damage at 355nm. The impurities on fused silica surface are detected by time-of-flight secondary ion mass spectrometry. The relative contents of metal-impurities and their distribution as a function of depth from the surface are acquired. Laser induced damage threshold and damage density are measured by a 9.3 ns (FWHM), tripled Nd:YAG laser. The impacts of impurities on laser induced damage of fused silica surface is analyzed. The results show that the contamination of magnetorheological finishing fuild also decreases damage performance of fused silica similar to conventional polishing powder. Strongly acidic solution can remove nearly all of metal impurities and no new contamination is introduced at the etching depth of 20 μm. The results can provide technique support for improving laser induced damage performance of fused silica.

1. Introduction

UV laser induced damage of fused silica optics limits the improvement of output capability in high power laser facility such as the National Ignition Facility in the United States [1,2], the Laser MegaJoule in France [3] and the SGIII laser facility in China [4,5]. Reports show that the intrinsic damage threshold of fused silica bulk material is higher than $100J/cm^2$ [6,7]. Laser-induced damage often occurs on the polished optical surface at fluences as low as a few J/cm^2 with nanosecond scale pulses. Literatures [8–15] show that the subsurface defects, which are introduced by manufactureing and buried under the optics surface, are responsible for igniting laser damage of conventional polished fused silica. There are two main kinds of defects in the subsurface of fused silica: highly absorptive contaminants resided in the Beilby layer or embedded in cracks [8-10] and subsurface cracks masked by Beilby layer [12-15].

In the past decade, the laser-induced surface damage resistance can be substantially increased through the removal of the subsurface defects by post processing treatment. Wet chemical etching [16-18] is an attractive way, having the advantages of: 1) potentially removing and mitigating the identified absorbing precursors leading to laser damage initiation; 2) globally treating the whole fused silica optic simultaneously; and 3) ultimately leading to less reliance on very challenging scratch/dig specifications on the finishing processes. However,

Battersby et al. [19] observed that further etching often results in a decrease rather than an increase in the damage threshold. Bude et al. [20] believed that salt contamination intrduced by etching solution may decrease the damage performance of fused silica. Another usual way is Magnetorheological finishing (MRF) [21-23]. MRF is usually used as a final polishing step that follows grinding and prepolishing. MRF uses magnetic carbonyl iron and nonmagnetic abrasive particles (diamond, cerium) mixed in water and some additives as polishing fluid. Since iron particles are magnetic, the rheology of the fluid can be modified by the application of a magnetic field. The removal of subsurface damage using MRF can be attributed to the small normal stress applied to the glass surface. So MRF has been described as an advanced polishing technique that can finish optics without propagating the subsurface damage layer. Unfortunately, residual contamination is inevitably introduced similar to conventional polishing processes during MRF processes.

This paper compares the residual impurities and their impacts on laser induced damage on fused silica surface processed by conventional polishing, MRF and wet chemical etching. Information of samples processed by different technics is given in Section 2. Polishing-induced impurities on fused silica subsurface are analyzed by time-of-flight secondary ion mass spectrometry (TOF-SIMS) in Section 3. Section 4 shows the damage testing procedure and its results. Section 5 is devoted to

the analyses and discussions of the obtained results and Section 6 draws the conclusions.

2. Sample preparation

Five 50mm×50mm×5mm fused silica samples were cutted from Heraeus Suprasil 312 blanks. They were manufactured using traditional chemo-mechanical polishing process by two vendors. After traditional polishing process, part samples of Vendor A and Vendor B were exposed to post processing to modify the amount of polishing induced contaminants in the polishing layer and SSD. In this procedure, three types of post processing were used: leaching in strongly acidic solution (HNO_3 and H_2O_2), acid etching in HF solution and magnetorheological finishing (MRF). Sample preparation methods are summarized in Table 1. Before damage testing and impurities analyses, all the samples were cleaned using the same cleaning procedure.

Table 1. Sample preparation methods

S/N	Slurry type	MRF	HNO_3 and H_2O_2	HF Etching
A1	CeO_2	No	No	No
A2	CeO_2	Yes, 5um, Carbonyl Iron	No	No
B1	CeO_2	No	No	No
B2	CeO_2	No	Yes	No
B3	CeO_2	No	Yes	20um

3. Impurities analyses

TOF-SIMS is a surface-sensitive analytical method that uses a pulsed ion beam to remove molecules from the very outermost surface of the sample. The particles removed from atomic monolayers on the surface are then accelerated into a "flight tube". Then their mass is determined by measuring the exact time at which they reach the detector (i.e. time-of-flight). Three operational modes are available using TOF-SIMS: surface spectroscopy, surface imaging and depth profiling. In this paper only depth profiling is considered. An ion gun is operated in the DC mode during the sputtering phase in order to remove material. A second ion gun is operated in the pulsed mode for acquisition phase. The analysis area of $100×100\mu m^2$ was randomly rastered by the primary ions with a spatial resolution of 1μm. Depth profiling by TOF-SIMS allows monitoring of all species of interest simultaneously with high mass resolution. All sample surfaces were sputter cleaned for twenty seconds to remove contaminations induced by surroundings.
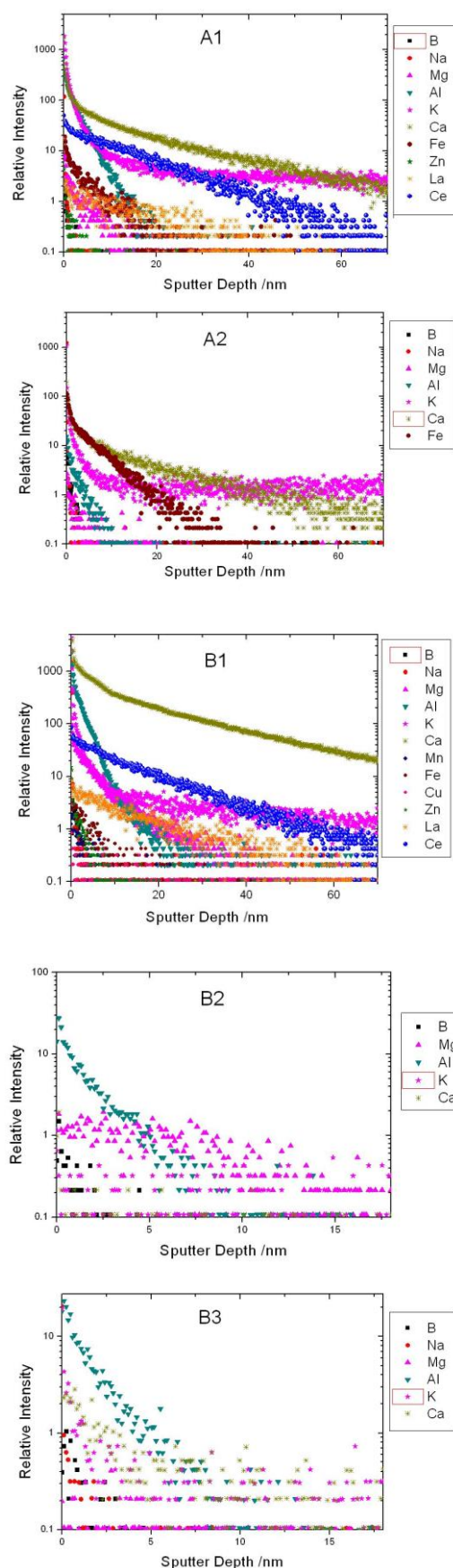

Fig. 1. The depth profiles of impurities detected on various samples subsurface by TOFSIMS

Table 2. The cumulated amount of impurities in the depth of 70 nm for our samples

S/N	B	Na	Mg	Al	K	Ca	Fe	Cu	Zn	La	Ce
A1	12	6932	133	5926	31533	13751	394	---	19	221	3182
A2	42	1252	32	157	2614	2711	1974	---	---	---	---
B1	37	2283	653	1123	1592	79931	46	22	11	494	3973
B2	7	95	4	236	26	8	---	---	---	---	---
B3	7	26	6	247	67	70	---	---	---	---	---

Depth profiles of impurities detected on various sample subsurface are shown in Fig. 1. The data had been normalized with silicon particle number (counts 10000) as a standard. The cumulated amount of each impurity in the depth of 70 nm is shown in Table 2. The nulls in Table 2 represent that we can not detect mass spectrum of these elements by TOF-SIMS. We can conclude that the kinds and amounts of impurities are varied for different process technics. There are many kinds of impurities (Na, Al, K, Ca, Fe and Ce etc) in the modified layer of traditional polishing fused silica. Because the polishing compound of Sample A1 and B1 is cerium oxide, many Ce impurities exist on the surface and subsurface. As the main constituent of polishing solution is carbonyl iron, magnetorheological finishing (Sample A2) can reduce the impurities content except Fe. After leaching in strongly acidic solution (HNO_3 and H_2O_2) and acid etching in HF solution, only small quantities of impurities exist on the surface of Sample B2 and B3. We stop testing for there are rarely impurities at the sputter depth of 30nm.

Fig. 1 show the diffusion depth of various impurities. The relative content of impurities has a slight effect to its diffusion depth, such as the diffusion depth of Fe is about 30nm for Sample A1 and 60nm for Sample A2. The main impurities with similar quantity, such as Na, K, Ca, Fe in Sample A2, Al and Ce in Sample A1, have different diffusion lengthes: Na's is no mre than 10 nm, Al's is about 20 nm, Fe's is about 50 nm, Ce's is about 70 nm, K's and Ca's are far more than 100 nm. These results suggest the thickness of modified layer is more than 100nm for traditional polsishing fused silica. The quantity and distribution of impurities have a relation to the processing technic of our samples.

4. Laser damage performance

An experimental setup of damage performance testing system is shown in Fig. 2. Continuum laser as a seed source is a single-mode YAG laser beam with 1064nm wavelength. It is amplified through amplifier and exports 355nm wavelength with 2J maximum output energy and 9.3ns pulse duration. The output energy is adjusted by using an energy attenuator. Telescope system is applied to filter high frequency modulation and reduce the diameter of beam. An uncoated fused silica pickoff wedge reflects two beams for the diagnostic systems. A calibrated pyroelectric detector measures pulse energy proportional to the energy at the sample under test location. A beam profiler placed at the same optical distance as the sample provides beam size and spatial profile information. A fast photodiode allows measurement of the temporal profile. The results are shown in Fig. 3, where a) is for laser pulse waveform and b) is for beam profile of testing area. An on-line microscopy with a pixel resolution of ~ 5μm detects rear surface damage.
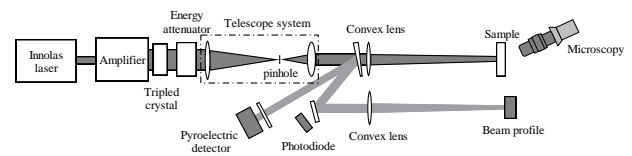

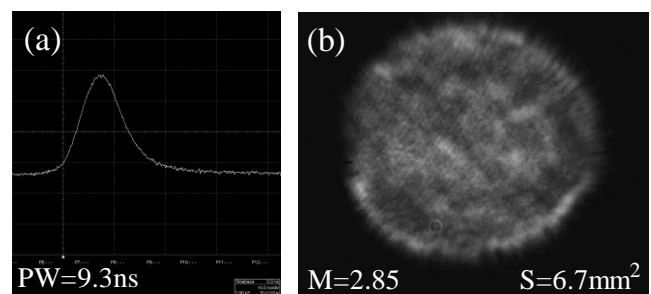*Fig. 2. Experimental setup of damage performance testing system.*

Fig. 3. Laser pulse waveform (a) and intensity distribution of flat top beam at target plane (b)

The spatial beam distribution shown in Fig. 3(b) is flat top beam with an effective diameter of ~3 mm. The modulation ratio in the effective area is 2.85. The damage fluence shown in this paper has been rescaled to a 3 ns pulse duration by using 1/2 law [7]. The average fluence has an absolute uncertainty of ± 5.6%. The damage threshold is measured with R on 1 procedure, in which the fluence is incrementally ramped with 0.6J/cm^2 step until damage is registered on the online microscopy. The damage probability at every fluence step is obtained. Fig. 4 shows the damage probability curve of samples in Table 1. Zero probability damage threshold can be deduced with the damage probability curve, as shown in Table 3. Zero probability damage threshold of fused silica samples is

from 5.93 J/cm^2 up to 11.58 J/cm^2. There is a huge difference between damage thresholds sugguesting various technological level of samples.
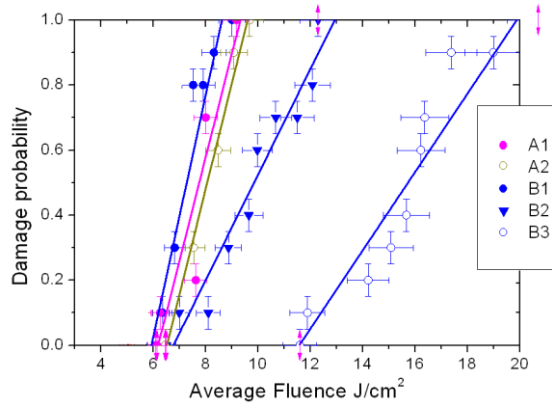

Fig. 4. Damage probability curve of various samples

Raster scan damage testing is applied to detect the optics damage density as a function of fluence using the same flat top beam. In order to have a good overlapping of the beam, we move continuously the sample along the x axis, and step by step along the y axis as shown in Fig. 5. Scan area is 10 cm^2 at same fluence. The modulation ratio of scanning area is about 2.8 with a comprehensive analysis of pulse-to-pulse fluence stability and beam overlapping. The automated damage detection system provides high resolution images of the sample surface immediately after each laser pulse. The damage sites number of scan area is acquired by image processing technology. Repeating this test at several fluences on different areas permits to determine the damage density versus average fluence. The damage densities of the samples versus average fluence are plotted in Fig. 6. The same as damage threshold, damage density exists difference between various samples. Laser-induced damage density at the average fluence of 6.5 J/cm^2 shown in Table 3 can be infered with the damage sensity versus fluence curve. The damage density listed in Table 3 is varied from 0.0015 to 0.32 damage sites per millimetre square at the average fluence of 6.5 J/cm^2.

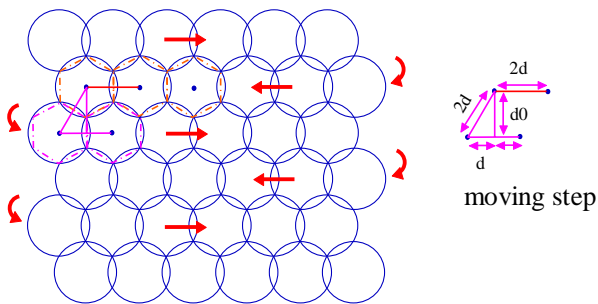*Fig. 5. Rasterscan procedure with a flat top beam. The moving step is 2d along the x axis and d0 along the y axis. In order to overlap the beam, moving ±d along the x axis is needed after moving d0 along the y axis*
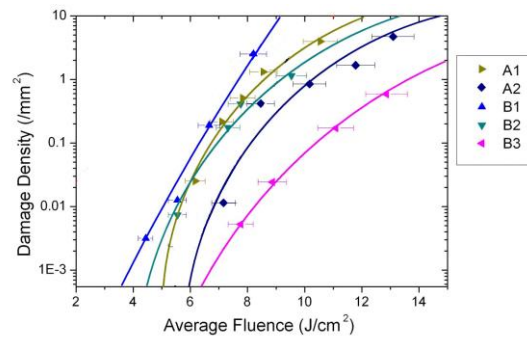

Fig. 6. Damage density versus average fluence of various samples

Table 3. Zero probability damage threshold and damage sites at the average fluence of 6.5J/cm^2 for our samples

	A1	A2	B1	B2	B3
Zero probability damage threshold (J/cm^2)	6.52	6.18	5.93	6.77	11.58
damage sites at the average fluence of 6.5J/cm^2 (/mm^2)	0.15	0.012	0.32	0.102	0.0015

We must illuminate that because the detector can't read out ~1μm which is the size of "gray haze", the "gray haze" damage can not be counted into damage density and considered as damage at damage threshold test [9, 24].

5. Discussion

The samples in this paper are divided into three types: traditional chemo-mechanical polished fused silica, acid etched fused silica and magnetorheological finished fused silica. Compared with traditional chemo-mechanical polished fused silica (Sample A1), Magnetorheological finished fused silica (Sample A2) shows that its surface has no Ce impurity and less other impurities except for Fe impurity increasing. The damage threshold of Sample A2 is near that of Sample A1, whereas the damage density at the average fluence of 6J/cm^2 is lower than Sample A1 one order of magnitude. We demonstrated in a previous work [24] that Ce imputity has a great influence on damage threshold while SSD density has a great influence on damage density. This suggests that the effects of surface impurities on laser damage performance are same for two Samples (A1 and A2) and magnetorheological polishing can reduce SSD effectively. Above analyses with the Sample A1and A2 show that not only Ce but also Fe has a serious influence on laser-induced damage. This agrees with our previous work [25] that Fe imputity also has a relation with laser damage threshold.

Acid etched fused silica Samples show that strongly acidic solution can remove nearly all of metal impurities. Comparing Sample B2 with Sample B1, we conclude that zero probability damage threshold is increased from 5.93 J/cm^2 to 6.77 J/cm^2 and damage density at the average fluence of $6J/cm^2$ is also decreased a little. The improvement of damage performance is attributed to the removal of metal impurities. In our perious work [26], we show that the "gray haze" damge disappear for strong acid leaching dissolving cerium element without modifying the subsurface damage. After acid etching in HF solution, Sample B3 has the similar impurities on its surface as Sample B2. But the damage performace increases amazingly: zero probability damage threshold increasing to 11.58 J/cm^2, damage density at the average fluence of $6J/cm^2$ decreasing two order of magnitude. It is not impurities but SSD that is responsible to the improvement [26-28]. The anlyses of impurities and laser damage performance show that there is not apparently new contamination during HF etching process.

6. Conclusion

We have represented the impurities and damage performance of fused silica under different polishing and post processing conditions. The correlations of damage performance with impurities are analyzed. The results show that iron impurity is introduced during MRF process and it has a serious influence on laser-induced damage. Strongly acidic solution can remove nearly all of metal impurities and HF acid etching can diminish subdurface damage effectively. The laser damage performance is increased amazingly at the etching depth of 20μm. It suggests no contamination introduced during HF etching process.

Acknowledgments

References

[1] E. I. Moses, J. H. Campbell, C. J. Stolz, C. R. Wuest, Proc. SPIE **5001**, 1 (2003).

[2] E. I. Moses, Proc. SPIE **5341**, 13 (2004).

[3] M. L. André, in Solid state lasers for application to Inertial Confinement Fusion: Second Annual International Conference, M. L. André, ed., Proc. SPIE **3047**, 38 (1996).

[4] H. S. Peng, X. M. Zhang, X. F. Wei, W. G., F. Jing, Z. Sui, Q. Zhao, D. Y. Fan, Z. Q. Ling, J. Q. Zhou, Proc. SPIE **4424**, 98 (2001).

[5] G. Y. Xiao, D. Y. Fan, S. J. Wang, Z. Q. Lin, Y. Gu, J. Q. Zhu, Y. X. Zhen, J. Zhu, F. Q. Liu, S. C. Chen, Q. H. Chen, G. L. Huang, X. M. Deng, Proc. SPIE **3492**, 890 (1998).

[6] T. A. Laurence, J. D. Bude, S. Ly, N. Shen, M. D. Feit, Opt. Express **20**(10), 11561 (2012).

[7] B. C. Stuart, M. D. Feit, S. Herman, A. M. Rubenchik, B. W. Shore, M. D. Perry, Phys. Rev. B Condens. Matter **53**(4), 1749 (1996).

[8] J. Neauport, P. Cormont, L. Lamaignére, C. Ambard, F. Pilon, H. Bercegol, Optics Communications **281**, 3802 (2008).

[9] J. Neauport, L. Lamaignere, H. Bercegol, Optics Express **13**, 10163 (2005).

[10] J. Huang, X. D. Zhou, H. J. Liu, F. R. Wang, X. D. Jiang, W. D. Wu, Y. J. Tang, W. G. Zheng, Opt. Engineering, **52**(2), 024203 (2013).

[11] F. R. Wang, H. J. Liu, J. Huang, X. D. Zhou, X. D. Jiang, W. D. Wu, W. G. Zheng, X. Ju, Chin. Phys. Lett., **28**(1), 014206 (2011).

[12] H. J. Liu, J. Huang, F. R. Wang, X. D. Zhou, X. D. Jiang, W. D. Wu, W. G. Zheng, Proc. of SPIE, **9255**, 92553V-1 (2015).

[13] F. R. Wang, H. J. Liu, J. Huang, X. D. Zhou, X. D. Jiang, W. D. Wu, W. G. Zheng, Acta Physica Sinica **59**(7), 5122 (2010).

[14] J. Neauport, P. Cormont, P. Legros, C. Ambard, J. Destribats, Optics Express **17**, 3543 (2009).

[15] F. Y. Génin, A. Salleo, T. V. Pistor, L. L. Chase, J. Opt. Soc. Am. A **18**, 2607 (2001).

[16] L. Wong, T. Suratwala, M. D. Feit, R. Steele, Journal of Non-Crystalline Solids **355**, 797 (2009).

[17] T. I. Suratwala, P. E. Miller, J. D. Bude, W. A. Steele, N. Shen, M. V. Monticelli, M. D. Feit, T. A. Laurence, M. A. Norton, C. W. Carr, L. L. Wong, J. Am. Ceram. Soc. **94**(2), 416 (2011).

[18] X. Jiang, Y. Liu, H. Rao, S. Fu, SPIE (2013).

[19] C. Battersby, L. Sheehan, M. Kozlowski, SPIE 3578 446 (1999).

[20] J. Bude, P. Miller, S. Baxamusa, N. Shen, T. Laurence, W. Steele, T. Suratwala, L. Wong, W. Carr, D. Cross, M. Monticelli, Optics Express, **22**(5), 5839 (2014).

[21] H. B. Cheng, Z. J. Feng, Y. W. Wang, J. Opt. Technol. **72**(11), 865 (2005).

[22] R. Catrina, D. Tarouxa, P. Cormonta, C. Mauniera, T. Corbineaua, G. Razéa, J. Néauport, SPIE 8884 88840A-1, 2013.

[23] R. Catrin, J. Neauport, D. Taroux, P. Cormont, C. Maunier, S. Lambertb, Optical Engineering **53**(9), 092010 (2014).

[24] H. J. Liu, J. Huang, F. R. Wang, X. D. Zhou, X. Ye, X. Y. Zhou, L. X. Sun, X. D. Jiang, Z. Sui, W. G. Zheng, Optics Express **21**, 12204 (2013).

[25] H. J. Liu, J. Huang, L. X. Sun, Q. Z. Li, X. Ye, F. R. Wang, F. Geng, X. D. Jiang, W. D. Wu, W. G. Zheng, Optoelectron. Adv. Mater. **17**(9), (2015).

[26] H. J. Liu, X. Ye, X. D. Zhou, J. Huang, F. R. Wang, X. Y. Zhou, W. D. Wu, X. D. Jiang, Z. Sui, W. G. Zheng, Opt. materials **36**, 855 (2014).

[27] T. I. Suratwala, P. E. Miller, J. D. Bude, W. A. Steele, N. Shen, M. V. Monticelli, M. D. Feit, T. A. Laurence, M. A. Norton, C. W. Carr, L. L. Wong, J. Am. Ceram. Soc. **94**(2), 416 (2011).

[28] J. Neauport, C. Ambard, P. Cormont, N. Darbois, J. Destribats, C. Luitot, O. Rondeau, Opt. Express **17**(22), 20448 (2009).

---

*Corresponding author: hongjie3713@163.com